sustainability

MDPI

Article

Effect of Ion Polarity Regime and Ventilation on Particle Removal Efficiency

Justinas Masionis *, Darius Čiužas, Edvinas Krugly, Martynas Tichonovas, Tadas Prasauskas, Justina Kukelkaitė and Dainius Martuzevičius

Department of Environmental Technology, Kaunas University of Technology, LT-50254 Kaunas, Lithuania; tadas.prasauskas@ktu.lt (T.P.)
* Correspondence: justinas.masionis@ktu.lt

Abstract

Ensuring the effective removal of airborne particles is essential for maintaining indoor air quality, particularly in environments with limited ventilation. This study examines how ion polarity regime, voltage, and relative humidity influence aerosol particle removal in a controlled, room-sized chamber (35.8 m^3) using a custom-built air ionizer. Experiments were conducted under stagnant and ventilated conditions (0.5 h^{-1}) while varying ionizer polarity (positive, negative, bipolar, alternating), voltage (6 kV, 10 kV), humidity (40%, 70%), and aerosol type (incense smoke, nebulized KCl). Positive and negative unipolar ionization achieved over 90% removal within 60 min, with decay rates of 0.04–0.05 min^{-1}, half-lives of 13–17 min, and clean air delivery rates (CADR) of 60–90 m^3 h^{-1}. Bipolar ionization was less efficient due to ion-ion recombination, yielding CADR values below 25 m^3 h^{-1}, while alternating polarity improved deposition (40–70 m^3 h^{-1}) by reducing recombination losses. Relative humidity had a minimal influence on unipolar performance but moderated efficiency in bipolar and alternating modes. Under low ventilation, unipolar negative ionization sustained high removal (96.7%), while ozone remained below the detection limits of the methods used. These findings indicate that ion polarity control and field strength strongly influence particle removal and that unipolar or alternating-polarity operation can provide effective particle removal under controlled chamber conditions, including a low-ventilation case of 0.5 h^{-1}.

Keywords: air ionization; particle deposition; ion polarity; clean air delivery rate; indoor air quality; ventilation

Academic Editor: Luca Stabile

Received: 30 March 2026
Revised: 21 May 2026
Accepted: 21 May 2026
Published: 25 May 2026

1. Introduction

Assuring good indoor air quality is an important public health task, given that people spend approximately 90% of their daily time indoors [1]. Indoor air pollution arises from both outdoor and indoor sources and is influenced by ambient air quality, building design, and occupant behavior. Common sources include cooking, heating, smoking, building materials, cleaning products, and personal care items. In rural or low-income areas, biomass combustion is a major contributor, whereas in urban environments, wildfire smoke and traffic emissions play a substantial role [2]. Biological aerosols, including bacteria, viruses, fungi, and pollen, are also important contributors to indoor air pollution. These bioaerosols originate from pets, plants, damp building materials, and HVAC systems, and are influenced by environmental factors such as humidity and temperature [3].

Indoor air pollution negatively impacts human health. It contributes to respiratory diseases, such as asthma and chronic obstructive pulmonary disease, and to cardiovascular issues, cancer, low birth weight, and neurological conditions. Health effects depend on pollutant concentration, exposure duration, and individual susceptibility. Additionally, polluting fuels like kerosene increase risks of burns, poisoning, and premature death, particularly in poorly ventilated homes [4].

To ensure safe indoor air, key strategies include pollutant source control, ventilation, and air purification [5]. Ventilation can be natural, mechanical, or hybrid [6]. Natural ventilation is energy-efficient but climate- and architecture-dependent, and often inadequate in polluted environments or poorly designed buildings [7]. Mechanical ventilation ensures reliable air exchange but increases energy use and emissions [8]. Hybrid systems combine both but require precise control and infrastructure [9]. Even with adequate source control and ventilation efforts, in some environments, controlling pollutant dispersion and human exposure remains challenging. In such cases, air purification technologies are needed.

Depending on the pollutants targeted, air purification methods include filtration, adsorption, UV irradiation, ionization, non-thermal plasma, membrane separation, and biofiltration [10–12]. Among these methods, filtration is the most widely used [12]. Particle phase pollutants are usually removed by mechanical filtration, which relies on fibrous media to remove particles by interception, impaction, diffusion and electrostatic attraction. However, it presents limitations such as pressure drop across the filter and thus energy consumption, as well as potential re-emission of pollutants if not maintained properly [13,14].

Particle removal with the help of electric field is classified into electrostatic precipitators (ESPs) and ionizers [11]. ESPs operate by charging particles in a high-voltage field and collecting them on electrodes [15,16]. They are integrated into HVAC systems or used as standalone units to capture particles with minimal pressure drop. Their efficiency depends on particle size, residence time, and electric field strength. Despite these advantages, ESPs are often associated with ozone release and struggle with capturing ultrafine particles (<50 nm) [15,17]. Their effectiveness can also be limited at higher flow rates that reduce residence time, especially in compact systems.

Air ionizers also utilize high voltage to create a flow of ions, but emit these outside the reactor into the air, thus using the volume of the compartment to attach to particles, inducing aggregation and promoting deposition. Negative air ions (NAIs) and positive air ions (PAIs) have lifespans of ~100 s and interact with environmental factors like humidity and temperature. NAIs mainly include superoxide ions (O_2^-) and hydroxide ions (OH^-), while PAIs include O_2^+, N^+, and H_3O^+ [18,19]. The health effects of air ions are debated, with some studies showing benefits [20–22], and others showing no clear effect [23,24].

The recent literature indicates that the performance of ionization-based air cleaning depends strongly on device design, ion output, airflow conditions, and the operating environment. Classroom-scale studies have reported limited particle removal by some bipolar ionizers compared with ventilation and HEPA filtration, together with possible by-product formation, whereas testing of ionization-type air purifiers under actual driving conditions has shown that practical performance should be interpreted together with ozone generation and compared against filtration-based alternatives [25,26]. A recent review of negative-air-ion-based purification in confined spaces further emphasized that aerosol removal is governed by ion generation, ion-particle attachment, electrostatic drift, surface deposition, and ventilation-dependent ion transport [27]. Recent work has also extended ionization research toward airborne microorganism control in room-scale environments [28].

However, despite growing recent interest, systematic evidence on ionizer performance is still relatively scarce. In particular, only a few studies have systematically examined how operational parameters, such as ion polarity (positive, negative, bipolar, and alternating),

voltage strength, and relative humidity, affect aerosol deposition rates, especially in room-sized environments relevant to indoor conditions. The present study addresses this gap through a systematic experimental evaluation of ionization operating parameters using a custom-designed air ionizer in a room-sized chamber. In addition to comparing positive and negative unipolar and bipolar operation, it investigates minute-scale alternating-polarity ionization as a comparatively underexplored operating mode for room-scale aerosol removal. In this way, the study clarifies the contribution of polarity regime, voltage, humidity, aerosol type, and ventilation condition to particle removal under controlled indoor conditions.

2. Materials and Methods

2.1. Test Chamber

The experiment was carried out in a test chamber simulating a typical room or office, with a floor area of 13 m^2 and a volume of 35.8 m^3. This chamber was installed within a 150 m^3 laboratory space. The experimental setup is shown in Figure 1. The walls, floor, and ceiling of the chamber were constructed using conventional building materials, including painted drywall, PVC floor lining, and a panel board ceiling.

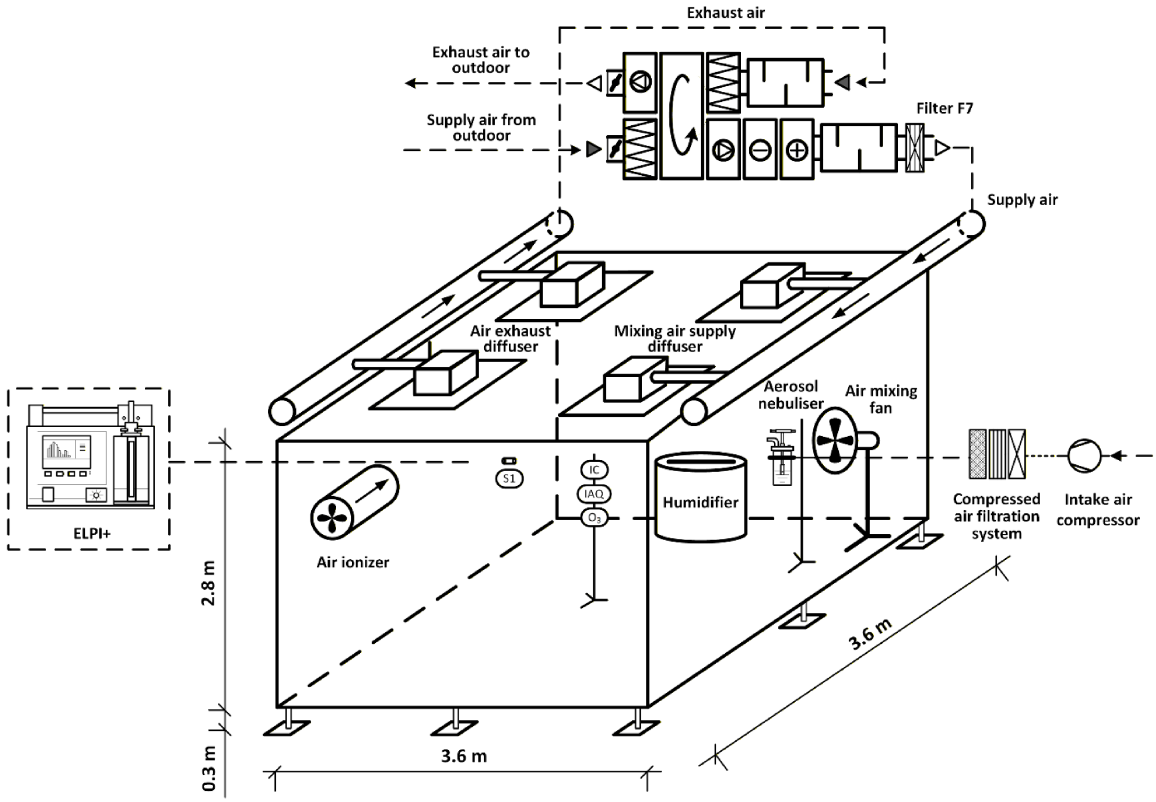

Figure 1. The schematic representation of test chamber employed for ionizer testing, equipped with air supply and exhaust system connected to an air handling unit with a heat exchanger: IC, ion counter; IAQ, indoor air quality meter (temperature, relative humidity and CO_2 concentration); O_3, real-time and colorimetric ozone detectors.

The chamber was equipped with an air supply system connected to an air handling unit (Gold04, Swegon, Stockholm, Sweden) featuring two in-ceiling diffusers for mixing ventilation, along with two in-ceiling exhaust diffusers. Additional air mixing and dispersion of generated pollutants were ensured using a fan. A Collison-type nebulizer for KCl suspension nebulization was placed in front of the fan, while the air ionizer was suspended from the ceiling on the opposite side of the chamber, at a height of 2 m.

Air samples were collected at location S1 (Figure 1) through the fixed chamber sampling port. Pre-experimental measurements performed at five locations in the chamber (four corners and the center) indicated that particle concentrations became sufficiently uniform within approximately 5 min after aerosol generation. In the sealed-chamber experiments, mixing was promoted by the auxiliary fan and the internal fan of the ionizer, whereas in the experiments conducted at 0.5 h^{-1}, the ventilation system additionally contributed to mixing. Therefore, S1 was used as a fixed point for tracking temporal concentration decay across all test conditions. An indoor air quality meter (7545 IAQ-CALC, TSI Inc., Shoreview, MN, USA) for measuring temperature, relative humidity, and CO_2 concentration, an ozone sensor with colorimetric tubes, and an air ion counter were placed in the center of the chamber for real-time monitoring of environmental parameters.

The chamber was installed in a laboratory setting where the ambient temperature was approximately 21 °C. Relative humidity inside the chamber was maintained at either 40% or 70%, depending on the experimental conditions, using a humidifier.

2.2. Air Ionizer

For the experiment, a custom-made air ionizer consisting of four independent ionization modules was used (Figure 2). Each module had a brush-to-tube configuration, with a thin tungsten wire brush positioned centrally inside a grounded stainless steel tube with a diameter of 100 mm. Each brush consisted of 18 tungsten wires, each 0.1 mm in diameter, with an approximate tip curvature radius of 0.05 mm. The wires were arranged radially from the center to form a semi-spherical brush geometry within the surrounding tube. All four ionization modules were mounted inside a stainless steel cylindrical housing with a diameter of 250 mm. Two in-house-built direct current power supply units were used to provide variable voltages (6 and 10 kV), each controlling one pair of electrodes. During unipolar ionization, all four electrodes were supplied with either positive or negative voltage. In bipolar mode, one pair generated positive ions and the other negative ions. In alternating mode, all four electrodes were charged unipolarly, with the polarity switching every 5 or 10 min. These switching intervals were selected as representative minute-scale cycles to test whether longer unipolar phases between reversals improve particle deposition under chamber conditions. Comparable literature on minute-scale alternating-polarity ionization for room-scale aerosol removal is limited. In contrast, alternating-polarity corona ionizers described in the literature are typically intended for electrostatic charge neutralization using rapid polarity switching rather than for chamber-scale particle removal [29]. The ionizer was equipped with an internal fan operating at a constant flow rate of 320 m^3 h^{-1}.

Before the experiments, ion concentration generated by the air ionizer was measured at a distance of 1 m from the emitters. The results are presented in Table 1.

Table 1. The production capacity of ions in the tested ionizer, represented as ion concentration measured 1 m downstream from the ionizer outlet airflow.

Ionizer Mode	Voltage, kV	Ion Concentration at 1 m from the Ionizer Outlet, $\times 10^6$ Ions cm^{-3}
Positive	6	17
	10	21
Negative	6	16.5
	10	19
Bipolar	6	30
	10	35

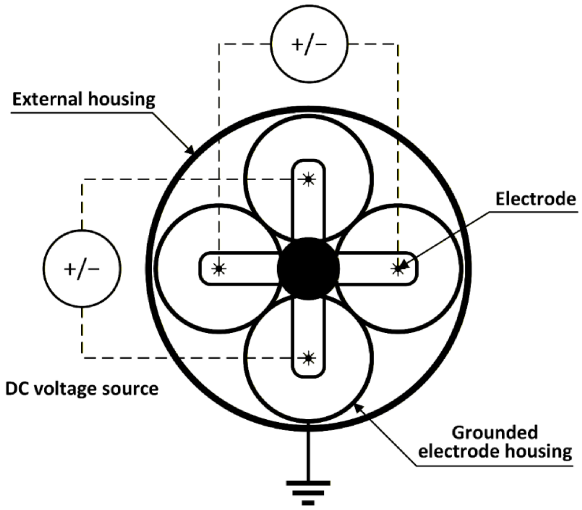

Figure 2. The schematic representation of the cross-section of the air ionizer used in this study, showing the electrode and DC power supply configurations.

2.3. Measurement of Aerosol Particle Concentration and Size Distribution

The real-time aerosol particle concentration and size distribution were measured using an Electric Low-Pressure Impactor (ELPI+, Dekati Ltd., Tampere, Finland). This instrument utilizes the cascade impaction principle and separates aerosol particles into 15 size fractions (0.006–10.0 μm) at a sampling flow rate of 10 L min^{-1}. Real-time aerosol particle number concentrations were recorded at 1 s intervals. After each measurement run, the ELPI+ baseline was checked in zero mode, and if baseline drift was observed, the instrument was re-zeroed before the next experiment. In addition, sampled air was passed through an 85 Kr bipolar (3054 A, TSI Inc., Shoreview, MN, USA) neutralizer before entering the ELPI+ to minimize potential effects of varying particle charging profiles during the experiments. Therefore, the ELPI+ measurements were used to evaluate particle concentration decay and size distribution, but not to preserve or characterize the native in-flight charge state of particles.

2.4. Air Change Rate Assessment

The natural air change rate inside the chamber was measured prior to the experiment using the CO_2 tracer gas decay method (ASTM E741) [30], with an indoor air quality meter. The rate was determined to be 0.017 h^{-1} (Figure S1), indicating a high level of chamber tightness. This sealed-chamber condition was used as a controlled baseline to assess ionization-driven particle removal in the absence of meaningful ventilation.

The experiment was conducted in two parts: the first part aimed at assessing the efficacy of the air ionizer without ventilation, and the second part combined with ventilation. For the experiments with ventilation, an air change rate of 0.5 h^{-1} was maintained by adjusting the air supply and exhaust rates. This was achieved by adjusting the diffuser openings and measuring the flow using an anemometer (Testo 417, Testo SE & Co. KGaA, Titisee-Neustadt, Germany).

2.5. Ion Concentration Measurement

Air ion concentration was measured using an air ion counter (AIC3Pro, AlphaLab, Inc., Pittsburgh, PA, USA). The device was placed in the middle of the room (Figure 1, IC) to enable real-time concentration monitoring and evaluation of ion saturation in the chamber, considering that the ion counter sampled air not directly exposed to the ionizer airflow direction.

2.6. O_3 Measurement

O_3 concentration potentially formed during each ionization stage was continuously monitored using an O_3 detector (GRI-9106-E-03, Hunan Guorui (GRI) Instrument Co., Ltd., Changsha, China) (Figure 1, O_3), with a detection limit of 100 ppb, and a colorimetric gas detection method using Ozone 0.05/b tubes (Dräger Nederland B.V., Zoetermeer, The Netherlands), with a detection limit of 50 ppb. Both methods yielded values below their detection limits during all test runs.

2.7. Generation of Aerosols

Two types of aerosols were used in the experiment to analyze the impact of air ionization on different particle size distributions and aerosol types: incense smoke (organic) and KCl nebulization (inorganic). Incense aerosol was generated by smoldering incense stick near air mixing fan (at the same position as the Collison nebulizer) for 1 min or until the total particle number in chamber reached 1.6×10^5 particles cm^{-3}. KCl 5% suspension was nebulized at the same location using Collison nebulizer (Model CN 24 J, BGI Inc., Cambridge, MA, USA) at 2 bar pressure for 15 min or until total particle number in chamber reached 1×10^5 particles cm^{-3}. Air for nebulization passed through a filter system (Figure 1) to avoid the introduction of additional pollutants into the chamber. Organic and inorganic aerosol particles were selected to represent the differences in their interaction with ions generated by the air ionizer due to variations in their composition, surface charge characteristics, and hygroscopicity [31,32].

2.8. The Experimental Design

The following parameters were varied during the experiment:

- Ionizer polarity: positive, negative, bipolar, alternating polarity with 5 and 10 min switching intervals;
- Ionizer voltage: 6 and 10 kV;
- Relative humidity: 40 and 70%, representing dry and humid environments;
- Aerosol type: incense smoke and KCl.

Each experimental condition was performed in three independent replicates, and the reported values represent the mean of these measurements. In the first part of the study, the chamber ventilation system was deactivated to isolate the effects of air ionization on particle deposition. As 5 kV represents the minimum threshold for initiating air ionization, a voltage of 6 kV was selected as the lowest operational setting to ensure consistent ion production, accounting for potential fluctuations in output. A maximum voltage of 10 kV was employed, as further increases were observed to intensify corona discharge, resulting in audible hissing and elevated ozone generation, which are considered undesirable for indoor applications. Relative humidity was maintained at 40% to assess ionizer performance under typical indoor environmental conditions. An elevated humidity level of 70% was additionally tested to replicate high-humidity environments such as those encountered in the food processing industry [33]. During each experiment, the ionizer exposure time was 60 min. The detailed experimental plan is shown in Table 2. The performance of different ionizer modes was calculated and compared using clean air delivery rate (CADR, $m^3\ h^{-1}$) and percentage decrease in total particle number (N) according to the following equations:

$$CADR = V(k_a - k_n) \quad (1)$$

where V is the room volume, k_a is the measured decay rate, and k_n is the natural decay rate.

$$N = \frac{(C_0 - C_n)}{C_0} \cdot 100\% \quad (2)$$

where C_0 is the initial particle number, and C_n is the total particle number at minute n.

Table 2. Experimental plan for evaluating air ionizer efficacy under chamber conditions.

Experiment Number	Type of Aerosol	Relative Humidity in Room, %	Ionizer Voltage, kV	Ionizer Mode	Duration to Achieve 50% Particle Number Reduction, min	Particle Number Reduction After 60 min, %	Particle Number Reduction After 60 min Excluding Natural Decay, %
1	Incense	40	-	Off	more than 60	42.5	-
2	Incense	40	10	Positive	13	93.8	51.3
3	Incense	40	10	Negative	12	95.3	52.8
4	Incense	40	10	Bipolar	42	61.5	19.0
5	Incense	40	10	Alt 5 min	14	89.8	47.3
6	Incense	40	10	Alt 10 min	11	91.8	49.3
7	Incense	40	6	Positive	15	91.9	49.4
8	Incense	40	6	Negative	12	93.6	51.1
9	Incense	40	6	Bipolar	39	62.4	19.9
10	Incense	40	6	Alt 5 min	16	86.3	43.8
11	Incense	40	6	Alt 10 min	17	85.4	42.9
12	Incense	70	-	Off	more than 60	44.1	-
13	Incense	70	10	Positive	13	95.4	51.3
14	Incense	70	10	Negative	13	93.4	49.3
15	Incense	70	10	Bipolar	27	69.4	25.3
16	Incense	70	10	Alt 5 min	11	90.5	46.4
17	Incense	70	10	Alt 10 min	12	90.3	46.2
18	Incense	70	6	Positive	13	91.9	47.8
19	Incense	70	6	Negative	12	91.9	47.8
20	Incense	70	6	Bipolar	47	56.6	12.5
21	Incense	70	6	Alt 5 min	17	81.2	37.1
22	Incense	70	6	Alt 10 min	14	84.3	40.2
23	KCl	40	-	Off	54	48.0	-
24	KCl	40	10	Positive	11	96.2	48.2
25	KCl	40	10	Negative	11	94.7	46.7
26	KCl	40	10	Bipolar	46	56.8	8.8
27	KCl	40	10	Alt 5 min	14	86.3	38.3
28	KCl	40	10	Alt 10 min	11	90.2	42.2
29	KCl	40	6	Positive	15	91.5	43.5
30	KCl	40	6	Negative	14	90.2	42.2
31	KCl	40	6	Bipolar	50	54.4	6.4
32	KCl	40	6	Alt 5 min	22	76.5	28.5
33	KCl	40	6	Alt 10 min	18	80.3	32.3
34	KCl	70	-	Off	56	46.4	-
35	KCl	70	10	Positive	11	94.7	48.3
36	KCl	70	10	Negative	10	95.6	49.2
37	KCl	70	10	Bipolar	59	50.5	4.1
38	KCl	70	10	Alt 5 min	15	83.6	37.2
39	KCl	70	10	Alt 10 min	10	89.8	43.4
40	KCl	70	6	Positive	15	90.4	44.0
41	KCl	70	6	Negative	15	90.2	43.8
42	KCl	70	6	Bipolar	more than 60	47.6	1.2
43	KCl	70	6	Alt 5 min	29	70.8	24.4
44	KCl	70	6	Alt 10 min	17	81.2	34.8

The experimental data were analyzed using Excel 365 (Microsoft Corporation, Redmond, WA, USA), the graphs were generated using OriginPro 2021 (OriginLab Corporation, Northampton, MA, USA), and the schematic illustrations were created using Visio Professional 2021 (Microsoft Corp.). In the second part of the study, the chamber ventilation system was activated, maintaining an air change rate of 0.5 h^{-1}, to assess the additional air quality improvements provided by the air ionizer in conjunction with mechanical ventilation.

3. Results and Discussion

3.1. The Removal of Particulate Matter by Various Air Ionization Modes

3.1.1. Unipolar Ionizer

Both positive and negative ionization substantially enhanced particle deposition compared with natural decay. Under background conditions, particle concentration decay rate was about 0.01 min^{-1} with a half-life of 70–75 min. Activation of the ionizer increased decay to 0.04–0.05 min^{-1}, shortened half-life to 13–17 min and yielded a CADR of 60–90 m^3 h^{-1}. Total deposition exceeded 90% within 60 min (Table 3; first row of Figure 3). The similarity between positive and negative polarity suggests that removal efficiency is governed primarily by ion emission rate rather than charge [34].

Table 3. Unipolar ionizer performance after 60 min.

Ionizer Mode	Voltage, kV	Aerosol	Relative Humidity, %	Particle Deposition Efficacy, %	Decay Rate, $\times 10^{-3}$ min^{-1}	Half-Life, min	CADR, m^3 h^{-1}	Ion Concentration, $\times 10^3$ Ions cm^{-3} (Positive; Negative)
Off	-	Incense	40	42.5	9.21	75.3	-	+4.16; −3.67
	-		70	44.1	9.70	71.5	-	+3.35; −1.81
	-	KCl	40	48.0	10.90	53.8	-	+2.21; −0.59
	-		70	46.4	10.40	66.7	-	+2.32; −1.06
Positive	6	Incense	40	91.9	41.82	16.6	70.1	+11.29; −0.00
	10			93.8	46.33	15.0	79.7	+16.01; −0.00
	6		70	91.9	41.94	16.5	69.3	+4.55; −0.00
	10			95.3	51.46	13.5	89.7	+17.90; −0.00
	6	KCl	40	91.5	41.00	16.9	60.4	+1.14; −0.00
	10			96.2	54.29	12.8	88.9	+2.10; −0.00
	6		70	90.4	39.13	17.7	61.7	+1.06; −0.00
	10			94.7	49.01	14.1	82.9	+1.10; −0.00
Negative	6	Incense	40	93.6	45.82	15.1	78.6	+0.69; −6.40
	10			95.3	50.90	13.6	89.6	+0.79; −9.26
	6		70	91.9	41.81	16.6	69.0	+0.54; −1.58
	10			93.4	45.28	15.3	76.4	+0.60; −10.08
	6	KCl	40	90.2	38.70	17.9	55.5	+0.57; −0.20
	10			94.7	48.85	14.2	77.3	+0.61; −0.63
	6		70	90.2	38.72	17.9	60.8	+0.64; −0.04
	10			95.6	52.19	13.3	89.8	+0.64; −0.04

In terms of the effect of ionizer voltage, at 6 kV, positive polarity achieved 91.9% (incense) and 91.5% (KCl) removal with half-life near 17 min and CADR about 65 m^3 h^{-1}. Raising voltage to 10 kV increased deposition to 93.8–95.4% for incense and 94.7–96.2% for KCl, while half-life shortened to 13–15 min and CADR reached 79–89 m^3 h^{-1}. The improvement reflects stronger electric field intensity and higher ion flux that enhanced diffusion charging and electrostatic drift of particles toward grounded surfaces. Negative polarity produced nearly identical performance. At 6 kV, deposition reached 91.9–93.6%, half-life 16–17 min, and CADR 55–78 m^3 h^{-1}. At 10 kV, efficiencies increased to 93.4–95.8%, half-life 13–15 min, and CADR 76–90 m^3 h^{-1}. During the first 30 min, incense removal was marginally faster (≈3–5%) under negative polarity, likely due to slightly higher mobility of O_2^- and OH^- ions, but the difference disappeared once ion concentrations became high.

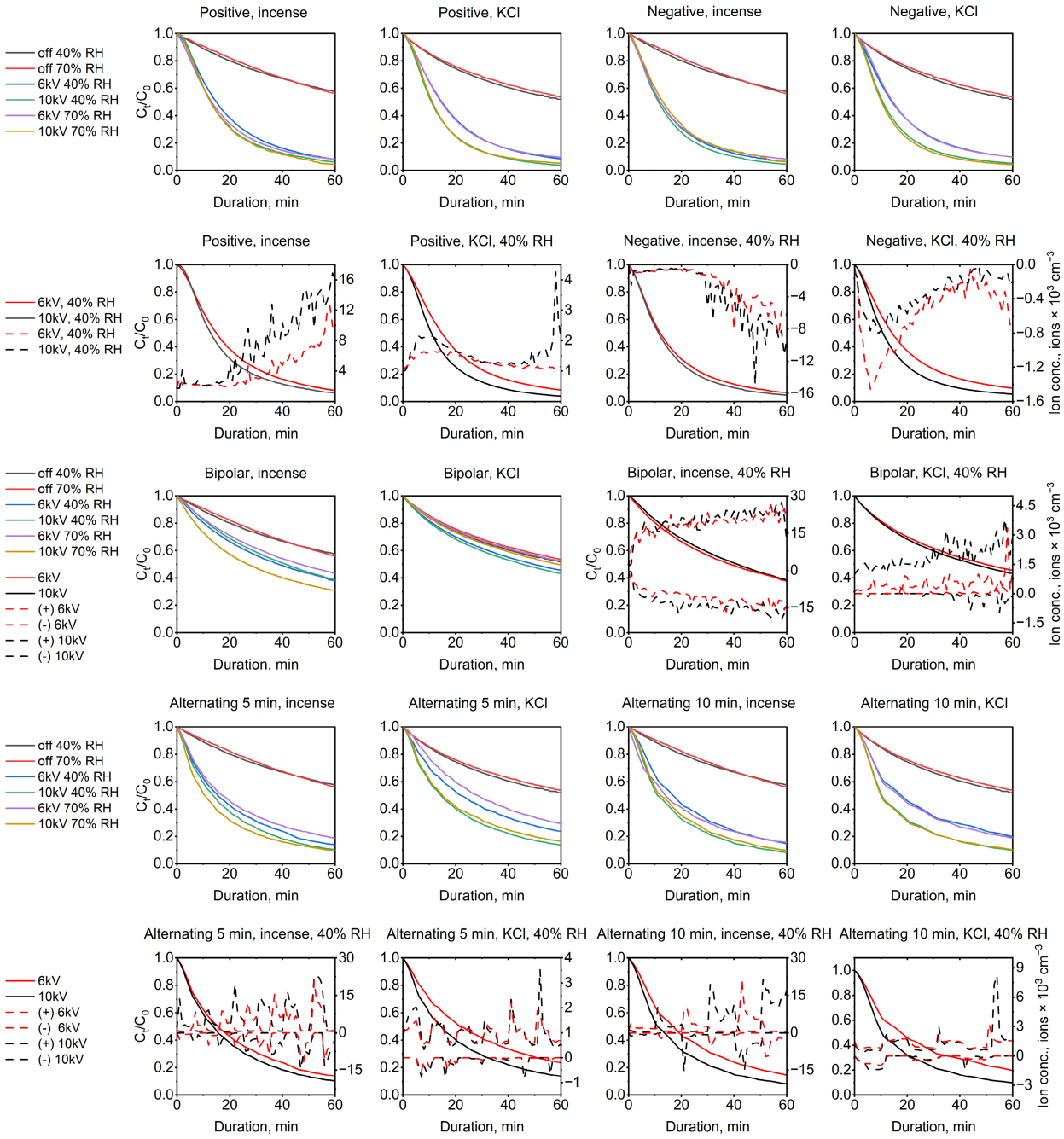

Figure 3. Normalized particle concentration of incense and KCl aerosols during exposure to different ionization regimes at 40–70% RH and applied voltages of 6–10 kV. Dashed lines indicate variations in ion concentration as a function of applied voltage and aerosol type at a constant RH of 40%. Random error, expressed as the coefficient of variation for repeated measurements (n = 3), ranged from 3 to 12% for C/C_0 and from 5 to 22% for ion concentration.

In contrast to the clear effect of voltage, relative humidity did not measurably influence particle removal under unipolar ionization in the present study. Previous studies indicate that relative humidity can influence ion-enhanced particle removal by modifying both electrostatic interactions and ion chemistry. In indoor environments, stronger electrostatic interactions are generally expected at lower RH, whereas at higher RH, moisture increasingly facilitates charge neutralization of particles and surfaces, with electrostatic interactions generally weakening as RH increases, and one study reporting a transition around 55% RH [35]. Room-scale ionizer studies have also identified RH as one of the

factors affecting ion-enhanced particle wall deposition, together with airflow, room size, ion concentration distribution, and wall properties [36]. From the ion-chemistry perspective, increasing humidity promotes hydration and clustering of ions in air, leading to the formation of hydrated positive and negative ion complexes, while also affecting ion-attachment and conversion processes in corona discharges. In addition, studies performed in ventilation ducts have shown that ionizer disinfection efficiency may decrease with increasing RH [37]. However, in the present study, no measurable difference in particle removal was observed between 40% and 70% RH under unipolar ionization. This suggests that, under the tested conditions, the humidity-driven microscopic changes in ion behavior were not large enough to alter the overall chamber-scale removal rate, which was likely dominated by the high ion output and airflow-driven particle transport.

Ion concentration and particle number showed correlating dynamics (second row of Figure 3) for both aerosol types. During aerosol generation, ion levels fell sharply, owing to ion scavenging by suspended particles [38]. After ionizer activation, ion concentrations increased in both cases but diverged thereafter. In the incense experiments, ion levels continued to rise throughout the 60 min exposure, whereas in KCl tests they began to decline after about 10 min. The difference indicates stronger ion scavenging in the presence of KCl aerosol, which was generated without drying and therefore entered the chamber in liquid form. Because KCl is highly hygroscopic, its particles likely retained more conductive behavior than incense aerosol, especially at higher RH, whereas incense smoke consisted mainly of less hygroscopic carbonaceous soot [39–41]. The contrast between these aerosols is therefore better interpreted in terms of particle phase state, hygroscopicity, and electrical conductivity rather than dielectric constant alone. Under ionization, the more conductive KCl aerosol likely redistributed charge more readily over the particle surface and scavenged ions more efficiently, while the carbonaceous incense aerosol interacted differently with ions, allowing greater free-ion accumulation in the chamber. Literature further suggests that aerosol material can influence ionization-assisted removal, although this effect is not always dominant across all systems [27]. Toward the end of the KCl experiments, ion concentration rose slightly again as most particles were removed and ion loss decreased. Despite these different ion-scavenging patterns, both aerosols still achieved comparable deposition (>90%), indicating that the material-dependent effects influenced the charging and scavenging dynamics more strongly than the final 60 min removal outcome.

Particle size distribution data supported this mechanism (Figure 4). Under natural decay, the incense aerosol size distribution shifted from 0.156 μm to 0.258 μm, indicating coagulation. Under unipolar ionization, the shift was smaller, showing that like-charged particles repelled each other and remained individually suspended until they were electrostatically deposited on nearby surfaces. Charged particles induced image charges on walls and ceilings, promoting drift and attachment; this accounted for the observed decay rates and their insensitivity to humidity. Because the chamber walls and floor included painted drywall and PVC, some charge accumulation on these surfaces during unipolar ionization is also possible. Previous studies have shown that ion-enhanced particle deposition depends on the electrical properties of indoor surfaces, including surface resistivity, and that electrostatic charges tend to remain longer on particles and surfaces at lower relative humidity, whereas increasing moisture facilitates charge neutralization [35,36]. However, wall surface potential was not measured directly in the present study, so this effect could not be quantified. No obvious late-stage slowdown in particle decay was observed within the 60 min test period, suggesting that, if wall charging occurred, it did not dominate the overall chamber-scale removal behavior under the tested conditions.

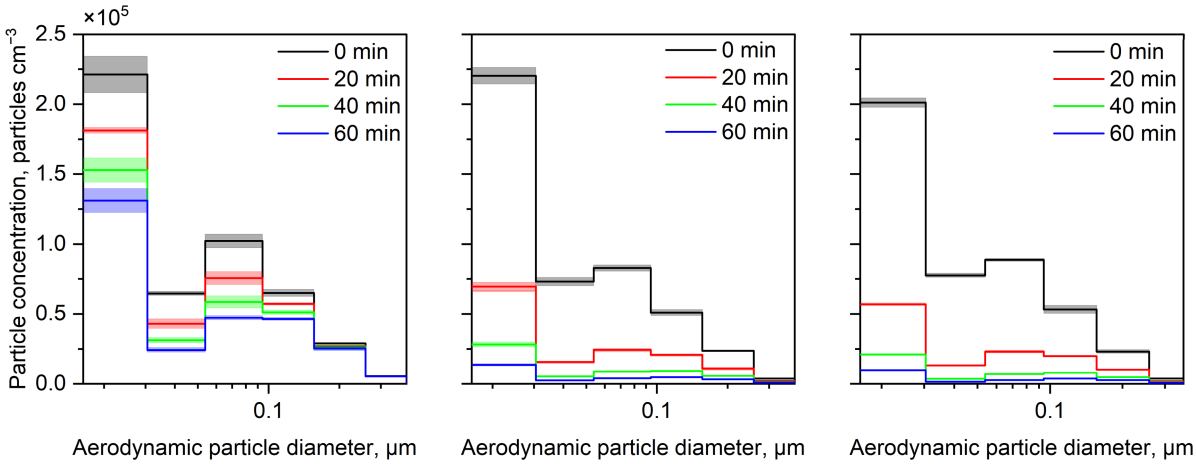

Figure 4. Incense aerosol size distribution at 40% RH during natural decay (**left**), positive air ionizer exposure (10 kV) (**middle**), and negative ionizer exposure (10 kV) (**right**).

Romay et al. (2024) [36] reported that unipolar ionizers increased particle deposition rate by about a factor of two using NaCl aerosol. The prototype used here produced a 4–5-fold increase, attributable to higher ion concentrations (1.7×10^7–2.3×10^7 ions cm^{-3} at 1 m) compared with 8×10^4 ions cm^{-3} at 1.35 m in their setup. Pushpawela et al. (2017) [42] likewise observed that ionizers, while less effective than HEPA filters in stagnant small chambers, outperformed them in ventilated rooms due to their spatially uniform ion distribution. They also found that ions could migrate through ventilation ducts and enhance deposition in adjacent spaces. The present results align with these findings, demonstrating that when ion flux is sufficiently high, unipolar ionization can achieve rapid, room-wide particle removal without mechanical filtration.

3.1.2. Bipolar Ionizer Performance

The bipolar ionizer was less efficient than the unipolar configuration, with particle removal lower by approximately 1.5–1.9 times under identical test conditions (Table 4; third row of Figure 3). The overall particle decay rate reached 0.01–0.02 min^{-1} compared with 0.04–0.05 min^{-1} in unipolar mode, corresponding to particle half-lives of 35–50 min and CADR between 2 and 22 m^3 h^{-1} depending on voltage, humidity, and aerosol type. The reduced performance is primarily due to ion-ion recombination, which lowers the concentration of free ions capable of charging particles and thereby weakens electrostatic drift toward grounded surfaces.

Table 4. Bipolar ionizer performance after 60 min.

Ionizer Mode	Voltage, kV	Aerosol	Relative Humidity, %	Particle Deposition Efficacy, %	Decay Rate, $\times 10^{-3}$ min^{-1}	Half-Life, min	CADR, m^3 h^{-1}	Ion Concentration, $\times 10^3$ Ions cm^{-3} (Positive; Negative)
Off	-	Incense	40	42.5	9.21	75.3	-	+4.16; −3.67
	-		70	44.1	9.70	71.5	-	+3.35; −1.81
Off	-	KCl	40	48.0	10.90	53.8	-	+2.21; −0.59
	-		70	46.4	10.40	66.7	-	+2.32; −1.06
Bipolar	6	Incense	40	62.4	16.30	42.5	15.2	+20.61; −14.17
	10			61.5	15.90	43.6	14.4	+10.81; −15.65
	6		70	56.7	13.93	49.8	9.1	+9.29; −8.09
	10			69.4	19.71	35.2	21.5	+18.27; −11.52
	6	KCl	40	54.4	13.09	53.0	0.4	+1.28; −0.07
	10			56.8	13.99	49.6	2.4	+2.95; −0.21
	6		70	47.6	10.76	64.4	0.8	+1.57; −0.00
	10			50.5	11.71	59.2	2.8	+1.72; −0.01

For KCl aerosol, deposition efficiency decreased slightly with increasing relative humidity from 54.4% to 47.6% at 6 kV and from 56.8% to 50.5% at 10 kV, while higher voltage improved removal modestly at both humidity levels. The increase in voltage raised ion flux and strengthened the electric field, which enhanced diffusion charging and drift forces, resulting in higher decay rates (from 0.01 to 0.02 min^{-1}), reduced half-life (from about 50 to 35 min), and CADR increasing from 0.4 m^3 h^{-1} at 6 kV to about 2.4 m^3 h^{-1} at 10 kV. The humidity dependence is plausibly related to the hygroscopic and conductive nature of KCl aerosol. At elevated RH, enhanced water uptake together with greater ion clustering and charge neutralization may have reduced effective particle charging and weakened electrostatic deposition [43]. Consequently, efficiency decreased at high RH despite the stronger field at 10 kV.

Incense aerosol exhibited a more pronounced and partly opposite response. Deposition increased with both voltage and humidity, from 12.5% at 6 kV and 40% RH to 25.3% at 10 kV and 70% RH, with decay rate rising from about 0.01 min^{-1} to 0.02 min^{-1}, half-life falling from 43 to 21 min, and CADR improving from 9 m^3 h^{-1} to over 21 m^3 h^{-1}. At 6 kV, the limited ion flux and higher recombination losses reduced the availability of small ions, which suppressed charging and caused a mild decrease in efficiency with humidity. At 10 kV, increased ion production overcame these losses and yielded a clear RH-related enhancement. This behavior reflects particle composition and phase: KCl remained conductive and less responsive to humidity, while incense, composed of dry, organic-rich ultrafine particles, softened at elevated RH, increasing surface adhesion and agglomeration upon contact with walls and thus promoting deposition.

Mechanistically, the bipolar ionizer produces both positive and negative ions simultaneously, which increases the probability of recombination near the emitters and within the chamber. This reduces the steady-state density of free ions and thus the net electrostatic driving force. The balance between diffusion charging, agglomeration, and recombination determines the overall deposition rate. At higher humidity, hydrated ions have lower mobility and form clusters, further reducing charging efficiency. Particle size data (Figure 5) support this mechanism: at 70% RH, the strongest decline occurred in the smallest size fractions (0.016–0.03 µm), with the secondary peak near 0.03 µm diminishing after 60 min. This indicates that ultrafine particles aggregated into larger particles, which were then deposited more efficiently. At 40% RH, size distributions changed little, consistent with weaker humidity-assisted agglomeration.

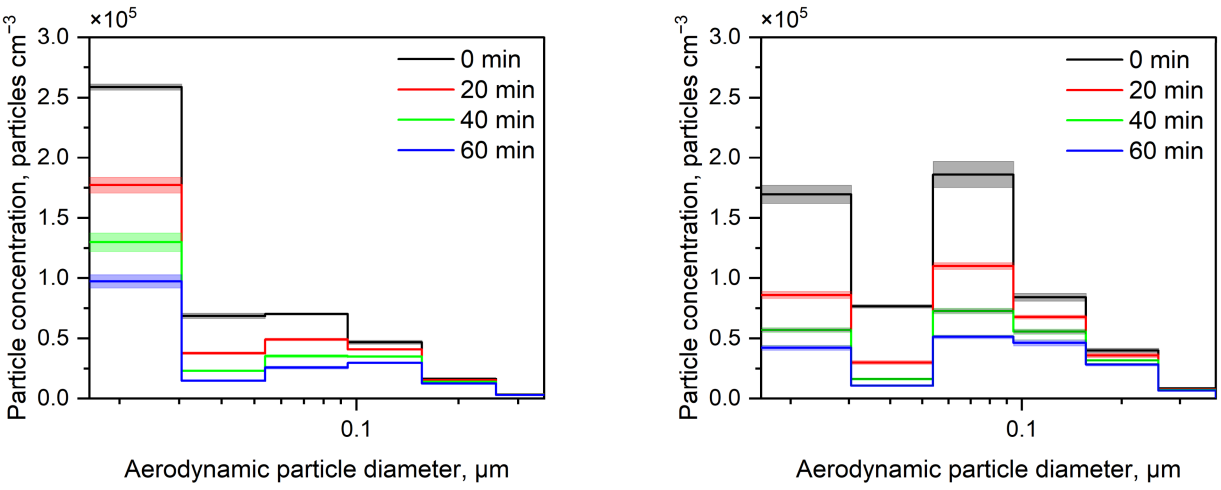

Figure 5. Incense particle size distribution during bipolar mode (10 kV) exposure at 40% (**left**) and 70% RH (**right**).

These results agree with previous chamber experiments. Kolarž et al. (2023) [44] found bipolar ionization to be two to three times less effective than unipolar negative operation across NaCl size fractions, largely due to lower ion concentrations (2×10^4 ions cm^{-3} at 2.5 m compared with 3.2×10^7 ions cm^{-3} at 1 m in this study). Zeng et al. (2021) [45] tested a bipolar ionizer in a 36.7 m^3 chamber (air change rate of 1.26 h^{-1}) and found negligible impact on $PM_{2.5}$ but an ≈ 11% increase in ultrafine particle removal, attributed to agglomeration. Their work also reported generation of oxygenated VOCs (acetone, butyraldehyde, ethanol, toluene) caused by corona discharge reactions. In follow-up work under full recirculation at 9 h^{-1}, Zeng et al. (2022) [46] again observed weak particle removal except when the ionizer was coupled with electret filters (MERV 10 or 13), where removal improved by about 8–10%.

3.1.3. Alternating Polarity

Alternating-polarity operation improved overall performance compared with continuous bipolar ionization by a factor of about 1.3–1.4, demonstrating its potential as a more effective approach when balanced exposure to both polarities is required (Table 5; Figure 3, fourth row). During alternating operation, the emitter periodically reversed polarity, producing sequences of positive and negative ions rather than simultaneous emission. This temporal separation reduced ion-ion recombination near the emitter and maintained a higher density of active ions in the air. The resulting field alternation also limited long-term charge buildup on surrounding surfaces and stabilized the overall electrostatic environment [47].

Table 5. Alternating-polarity ionizer performance after 60 min.

Ionizer Mode	Voltage, kV	Aerosol	Relative Humidity, %	Particle Deposition Efficacy, %	Decay Rate, $\times 10^{-3}$ min^{-1}	Half-Life, min	CADR, m^3 h^{-1}	Ion Concentration, $\times 10^3$ Ions cm^{-3} (Positive; Negative)
Off	-	Incense	40	42.5	9.21	75.3	-	+4.16; −3.67
	-		70	44.1	9.70	71.5	-	+3.35; −1.81
Off	-	KCl	40	48.0	10.90	53.8	-	+2.21; −0.59
	-		70	46.4	10.40	66.7	-	+2.32; −1.06
Alt 5 min	6	Incense	40	86.3	33.11	20.9	51.3	+0.59; −3.16
	10			89.8	37.98	18.3	61.8	+0.68; −6.44
	6		70	81.2	27.89	24.9	39.1	+0.51; −0.24
	10			90.5	39.21	17.7	63.4	+0.87; −7.47
	6	KCl	40	76.5	24.14	28.7	24.2	+0.67; −0.00
	10			86.3	33.07	21.0	43.4	+0.56; −0.00
	6		70	70.8	20.49	33.8	21.7	+0.64; −0.12
	10			83.6	30.18	23.0	42.5	+0.60; −0.07
Alt 10 min	6	Incense	40	85.4	32.01	21.7	49.0	+0.61; −2.48
	10			91.8	41.75	16.6	69.9	+17.19; −0.00
	6		70	84.3	30.85	22.5	45.4	+0.60; −1.40
	10			90.3	38.80	17.9	62.5	+0.57; −1.76
	6	KCl	40	80.3	27.08	25.6	30.5	+1.51; −0.00
	10			90.2	38.74	17.9	55.6	+1.46; −0.00
	6		70	81.2	27.83	24.9	37.4	+1.10; −0.00
	10			89.8	37.97	18.3	59.2	+1.67; −0.00

When the polarity was switched every 5 min, incense aerosol concentrations decreased by 81–90%, corresponding to particle decay rates of 0.03–0.04 min^{-1}, half-lives of 18–25 min, and CADR between 39 and 63 m^3 h^{-1}. Increasing the alternation period to 10 min yielded a small additional gain, with reductions of 84–92%, half-lives of 16–22 min, and CADR rising to 46–70 m^3 h^{-1}. Performance improved with voltage at both switching frequencies but showed limited sensitivity to humidity, except at 6 kV and 70% RH where efficiency decreased by about 5%. For KCl aerosol, efficiency also increased with voltage, though deposition weakened at higher humidity. These effects mirror those observed for unipolar operation, where enhanced ion flux increased diffusion charging, but high humidity promoted ion clustering and lowered ion mobility.

Mechanistically, alternating polarity creates alternating phases of unipolar ionization separated by brief recombination intervals. When the polarity reverses, newly generated ions neutralize residual ions of opposite charge remaining in the air, leading to transient loss of active ions and a short reduction in deposition rate. However, this recombination occurs only during switching rather than continuously as in bipolar mode, so overall efficiency remains higher. Between reversals, the chamber experiences unipolar-like conditions that allow particles to charge uniformly and deposit through electrostatic drift. The periodic polarity change also reverses image charge polarity on room surfaces, reducing charge accumulation and improving long-term charge balance.

Humidity influenced incense and KCl aerosols differently because of their contrasting physicochemical properties. Incense aerosol consists mainly of carbonaceous particles and is relatively less hygroscopic, whereas KCl aerosol is hygroscopic and can take up water as RH increases [39–41]. For KCl aerosol, higher RH may therefore have introduced two competing effects: hygroscopic growth of the particles and weakening of electrostatic interactions due to enhanced charge neutralization on particles and surfaces at elevated moisture levels [35,39]. The slight tendency toward lower KCl removal efficiency at higher RH is thus more plausibly interpreted as the net result of these opposing effects under the present conditions, rather than as evidence of a single dominant mechanism. In contrast, humidity-related changes for incense aerosol were likely smaller because its less hygroscopic carbonaceous particles interacted differently with water and ions. The dependence on voltage reflects ion flux and field strength, with the 10 kV configuration maintaining higher deposition rates and shorter particle half-lives across both aerosol types.

Comparable data are scarce in the literature, as most prior research on alternating-polarity ionization concerns electrostatic discharge control rather than air cleaning [48,49]. In such industrial systems, AC ionizers alternate polarity every millisecond, while pulse-DC devices switch every 1–10 s to maintain quasi-neutral charge environments. For air cleaning, the minute-scale alternation applied here appears more effective, providing enough time for unipolar charging and drift before polarity reversal. Shi & Ekberg (2015) [49] reported that periodic polarity switching restored and maintained filter efficiency by reversing accumulated charges on both particles and filter fibers, allowing continued capture of oppositely charged dust while keeping the pressure drop 25–30% lower than that of a higher-grade static filter.

3.2. Ionizer Performance Under Low Ventilation Conditions

While the previous sections evaluated ionizer performance in stagnant air, this experiment aimed to assess its effectiveness under low air exchange conditions, representing more realistic indoor environments. The negative ionizer operating at 10 kV, identified as the most efficient configuration in earlier experiments, was selected for testing. The air change rate was set to 0.5 h^{-1}, the relative humidity to 40%, and the temperature to 21 °C, corresponding to typical residential ventilation levels [50] and indoor environmental parameters [51]. Under these conditions, aerosol concentration decreased by 29.5% due to ventilation alone compared to natural decay, while ionization alone reduced airborne particle concentration by 95.3%. The combined ventilation and ionization condition resulted in a marginally higher particle removal of 96.7% at an air change rate of 0.5 h^{-1} after 60 min of exposure (Figure 6). These results indicate that, under the present chamber conditions, ionization provided stronger particle removal than low ventilation alone. However, this comparison applies only to aerosol particle concentration, since ventilation also performs broader indoor air quality functions, including control of CO_2 and gaseous pollutants. Thus, ionization should be regarded as a supplementary particle-control approach rather than a replacement for ventilation. Low ventilation also did not substantially reduce

ionization-driven particle removal under the tested conditions, supporting its potential use as a supplementary particle-control approach in environments with restricted air exchange.

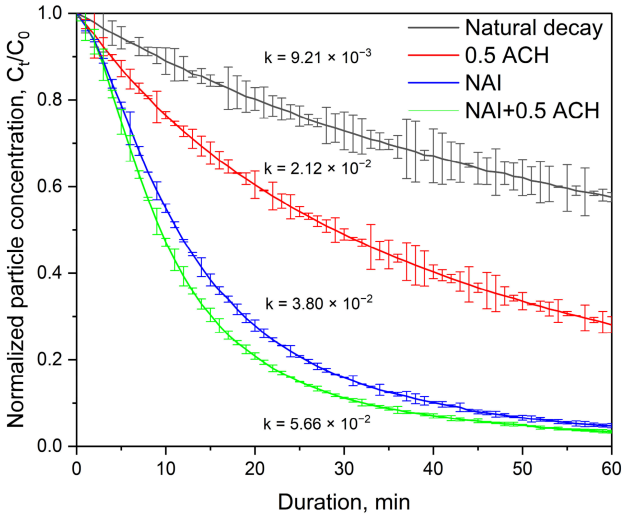

Figure 6. Negative ionizer (NAI) performance alone and in combination with ventilation at an air change rate of 0.5 h^{-1}, compared with the natural decay of incense aerosol. Values of k indicate the concentration decay rate (min^{-1}).

Fletcher et al. (2008) [52] analyzed ion concentrations in a ventilated room (32 m^3) and found that the ion levels generated by negative or bipolar ionizers remained nearly constant despite changes in the ventilation rate between 3 and 12 h^{-1}. The authors attributed this stability to the dominance of ion-ion recombination and electrical deposition on surfaces, which occur at rates substantially faster than ion removal through ventilation under steady-state conditions. In our study, the concentration of negative air ions slightly decreased at 0.5 h^{-1} compared to the condition without ventilation (Figure 7). These measurements were performed in the presence of incense aerosol, and the small deviation in ion concentration observed between separate measurements may have resulted from variations in aerosol concentration rather than from ventilation itself. At 0 h^{-1}, larger short-term fluctuations were observed, which can be explained by natural diffusion dominating under stagnant air conditions, leading to uneven ion distribution in the chamber.

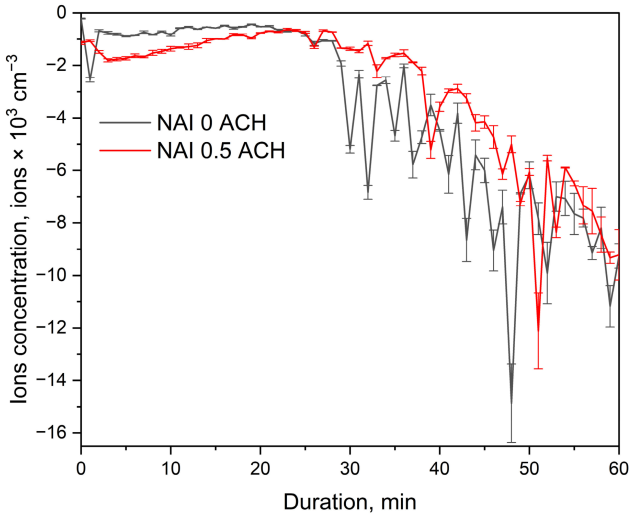

Figure 7. Negative ion concentration during experiments under stagnant conditions (0 h^{-1}) and at 0.5 h^{-1} with incense aerosol present in the chamber air.

3.3. Comparison with Published Chamber Studies on Ionizer Performance

Several studies have examined the performance of air ionizers in chambers of different sizes and ventilation regimes (Table 6). Most large-scale experiments have found that bipolar ionizers provide little or no improvement in particle removal, regardless of the applied air change rate. Zeng et al. (2021) [45] and Zeng et al. (2022) [46] reported negligible enhancement of aerosol decay by a needlepoint bipolar ionizer tested in a 36.7 m^3 chamber operating first in single-pass mode (1.26 h^{-1}) and then under full air recirculation (9 h^{-1}). Only a modest increase of about 8–10% in $PM_{2.5}$ removal was observed when the ionizer was combined with electret HVAC filters (MERV 10 or 13) during multi-pass operation. The weak effect likely reflects low ion densities and strong dilution at high ventilation rates, which limit charge transfer and deposition.

Table 6. Comparison of air ionizer performance in chamber studies reported in the literature.

Reference	Ionizer Polarity	Aerosol	Chamber Volume, m^3	Air Change Rate, h^{-1}	Combination with Filter	Aerosol Number Reduction, %	Exposure Duration, min	Measured Particle Size Range	CADR, m^3 h^{-1} (CADR/V, h^{-1})
This study	Positive	Incense	35.8	0.017	No	93.8	60	0.016–9.94 µm	79.7 (2.23)
		KCl				96.2			88.9 (2.48)
	Negative	Incense				95.3			89.6 (2.50)
		KCl				94.7			77.3 (2.16)
	Bipolar	Incense				61.5			14.4 (0.40)
		KCl				56.8			2.4 (0.07)
	Alt 5 min	Incense				89.8			61.8 (1.73)
		KCl				86.3			42.5 (1.19)
	Alt 10 min	Incense				91.8			69.9 (1.95)
		KCl				90.2			55.6 (1.55)
	Negative	Incense		0.5		96.7			101.8 (2.84)
[53]	Bipolar	Research-grade cigarettes	28	6	MERV 10	99 (mass)	40	0.35 µm	-
[45]	Bipolar	Incense	36.7	1.26	No	11 3	~240	0.01–0.15 µm 0.3–10 µm	- -
[46]	Bipolar (in-duct)	Ambient	36.7	1.8–2	No	Negligible	240	PM2.5	-
		Incense			No	Negligible	1440 (24 h)		-
					MERV 10 or 13	8–10 (ions added effect)			-
[25]	Bipolar (4 different)	NaCl	368	1.3	No	0	90	>0.5 µm	0.0 (0.00)
[42]	Negative	Ambient particles	30	3.4 *	No	40	15	0.02–1.0 µm	-
			45	2.4 *	No	30			-
			130	0.8 *	No	22			-
[54]	Negative	Cigarette	73.9	-	No	90	165	PM10	-
[36]	Positive	NaCl	57.1	5.1 *	No	50 (mass)	40	-	17.5 (0.31)
	Negative				No	50 (mass)	35		22.8 (0.40)
	Bipolar				No	0	-		0.0 (0.00)

* Recalculated using the parameters given in the article.

Farahi (2023) [53] studied a similar bipolar device (GPS NPBI^{TM}) in a 28 m^3 chamber equipped with a MERV 10 electret filter (Aeolus Filter Corporation, Archdale, NC, USA) in a recirculating HVAC loop operating at an air change rate of 6 h^{-1}. Cigarette smoke was used as a challenge aerosol. The addition of the ionizer increased filter performance approximately 16-fold, achieving removal efficiencies comparable to HEPA filtration. The ionizer produced about 2×10^4 ions cm^{-3}. Compared with [46], the ion concentration in Farahi's setup was about 47% higher, and the chamber volume was smaller, conditions that likely amplified ion-particle collision frequency and improved removal. The contrast between these studies illustrates that ionizer effectiveness scales with ion density and inversely with ventilation-induced dilution.

Gord et al. (2023) [25] evaluated several bipolar ionizers designed for in-duct installation in an unoccupied classroom (363 m^3). The ionizers were operated in short test ducts with fans simulating in-duct flow but not connected to the room's ventilation system. NaCl aerosol was continuously generated to maintain steady-state concentration at an air change

rate of 1.3 h^{-1} (>200 particles cm^{-3}). None of the ionizers measurably enhanced particle removal, confirming that ionization was ineffective in large, well-ventilated spaces with low baseline particle loading. Two devices slightly increased ultrafine particle counts (<10 nm), suggesting new particle formation likely associated with ozone-related reactions. These results indicate that low ion lifetimes and ozone chemistry can offset any potential benefit of ionization in large, well-mixed environments.

Unlike bipolar systems, unipolar ionizers generally show measurable benefits for particulate removal in large chambers. Pushpawela et al. (2017) [42] found a fanless negative ionizer more effective than a HEPA-based purifier in ventilated rooms of 30, 45, and 130 m^3 at 3.4, 2.4, and 0.8 h^{-1}, respectively. Within 15 min, particle concentrations decreased by 40%, 30%, and 22%, respectively. The lower performance in the smallest room relative to our study can be attributed to the absence of forced airflow, which limited ion dispersion and reduced the residence time of charged particles near the electrodes.

Černecký et al. (2015) [54] examined a DEZOSTER ionization system that delivered ionized air from a separate control chamber into a positively pressurized test space via ceiling diffusers. Air was exhausted at 0.6 m s^{-1}, maintaining forced ventilation. Cigarette smoke generated 3 m from the diffusers decreased by 90% in PM_{10} concentration within 165 min. The ionized environment accelerated particle decay by a factor of about 2.5 compared with natural conditions. However, when the source-to-diffuser distance increased to 4.5 m, performance dropped sharply, likely due to ion neutralization and wall losses, which reduced the effective ion concentration. Ion levels in that study (≈200 ions cm^{-3}) were several orders of magnitude lower than those in the present work (≈10^7 ions cm^{-3}), explaining the localized rather than room-wide effect.

Literature comparisons indicate that ionization performance is governed by ion density, spatial distribution, and air mixing intensity. In large or well-ventilated chambers, rapid ion recombination and dilution limit effectiveness, particularly for bipolar devices. In smaller or semi-confined spaces, especially under unipolar or alternating-polarity operation, ion concentrations sufficient to enhance deposition can be achieved, producing particle removal rates several times faster than natural decay. The present study supports these observations quantitatively. Under unipolar ionization, particle decay rates reached 0.04–0.05 min^{-1}, corresponding to half-lives of 13–17 min and CADR of 60–90 m^3 h^{-1}, approximately four to five times faster than natural decay. Alternating-polarity operation achieved decay rates of 0.03–0.04 min^{-1}, half-lives of 17–25 min, and CADR values of 40–70 m^3 h^{-1}, whereas bipolar ionization remained substantially less efficient, with decay rates of 0.01–0.02 min^{-1} and CADR below 25 m^3 h^{-1}. These findings confirm that maintaining a predominance of one ion polarity in the air, either continuously or sequentially, minimizes recombination losses and maximizes particle charging efficiency. The high removal efficiencies observed here were achieved at ion concentrations of 1.7×10^7 to 2.3×10^7 ions cm^{-3} within a room-sized chamber, a range consistent with conditions expected to promote measurable electrostatic drift. Ionizer performance scales nonlinearly with ion concentration and is strongly constrained by air exchange rate, voltage level, and emission geometry, supporting the conclusion that effective application of ionization for indoor air cleaning requires both controlled field intensity and spatially uniform ion distribution.

4. Conclusions

This study investigated the influence of ion polarity, voltage, and relative humidity on aerosol particle deposition efficiency under controlled indoor conditions. Both positive and negative unipolar ionization achieved stable deposition efficiencies above 90%, particle half-lives of 13–17 min, and CADR values of 60–90 m^3 h^{-1}. Efficiency scaled with voltage but remained independent of humidity or aerosol composition. In confined indoor air,

particle removal is therefore controlled by ion concentration and field strength rather than by charge polarity.

Bipolar ionization yields moderate and humidity-sensitive particle removal, resulting in decay rates of only 0.01–0.02 min^{-1}, half-lives of 30–50 min, and CADR values below 25 m^3 h^{-1}. Compared with unipolar operation, it remained roughly twofold less efficient, which can be attributed to the intrinsic loss of charge through continuous recombination of oppositely charged ions.

Alternating-polarity operation achieved decay rates of 0.03–0.04 min^{-1}, particle half-lives of 17–25 min, and CADR values of 40–70 m^3 h^{-1}, substantially exceeding the performance of bipolar ionization but still slightly below that of continuous unipolar operation. The alternating-polarity ionization functions as a sequential unipolar process with periodic charge reversal, maintaining effective particle removal while minimizing residual surface charge buildup in indoor environments.

Under typical residential ventilation conditions of 0.5 h^{-1}, the ionizer operating in negative mode maintained high performance, achieving a 96.7% reduction in incense aerosol concentration after 60 min of exposure. This indicates that, under the tested low-ventilation condition of 0.5 h^{-1}, ionization-driven particle removal remained effective and substantial particle reduction could be sustained.

The study demonstrated the potential of ionization as an effective approach for improving indoor air quality. The presented ionization regimes may be adapted for integration into residential or commercial ventilation units, where varying unipolar or alternating-polarity operation may enhance particle removal with reduced static charge buildup and controlled ozone emission. In addition, ionization may also be considered as a supplementary technology used together with HVAC filtration systems to support particle removal under suitable operating conditions. Future work will focus on a more detailed evaluation of ozone formation, ion production, and biological effects under different polarity regimes and electrode configurations, in order to better define the relationship between air-cleaning efficacy, microbial inactivation, and byproduct generation.

Supplementary Materials: The following supporting information can be downloaded at https://www.mdpi.com/article/10.3390/su18115305/s1. Figure S1. Natural air change rate in the chamber, using CO_2 as tracer gas.

Author Contributions: J.M.: Investigation, Data curation, Methodology, Visualization, Writing—original draft. D.Č. and M.T.: Data curation, Validation. E.K.: Data curation, Writing—review and editing, Formal analysis. T.P.: Investigation, Data curation. J.K.: Investigation; D.M.: Conceptualization, Data curation, Formal analysis, Supervision, Writing—review and editing. All authors have read and agreed to the published version of the manuscript.

Funding: This research received no external funding.

Institutional Review Board Statement: Not applicable.

Informed Consent Statement: Not applicable.

Data Availability Statement: The data that support the findings of this study are available from the corresponding author, [Justinas Masionis], upon reasonable request.

Conflicts of Interest: The authors declare that they have no known competing financial interests or personal relationships that could have appeared to influence the work reported in this paper.

References

1. Schweizer, C.; Edwards, R.D.; Bayer-Oglesby, L.; Gauderman, W.J.; Ilacqua, V.; Juhani Jantunen, M.; Lai, H.K.; Nieuwenhuijsen, M.; Künzli, N. Indoor Time-Microenvironment-Activity Patterns in Seven Regions of Europe. *J. Expo. Sci. Environ. Epidemiol.* **2007**, *17*, 170–181. [CrossRef]

2. Radbel, J.; Rebuli, M.E.; Kipen, H.; Brigham, E. Indoor Air Pollution and Airway Health. *J. Allergy Clin. Immunol.* **2024**, *154*, 835–846. [CrossRef]
3. Kumar, P.; Kausar, M.A.; Singh, A.B.; Singh, R. Biological Contaminants in the Indoor Air Environment and Their Impacts on Human Health. *Air Qual. Atmos. Health* **2021**, *14*, 1723–1736. [CrossRef]
4. Kumar, P.; Singh, A.B.; Arora, T.; Singh, S.; Singh, R. Critical Review on Emerging Health Effects Associated with the Indoor Air Quality and Its Sustainable Management. *Sci. Total Environ.* **2023**, *872*, 162163. [CrossRef]
5. Luengas, A.; Barona, A.; Hort, C.; Gallastegui, G.; Platel, V.; Elias, A. A Review of Indoor Air Treatment Technologies. *Rev. Environ. Sci. Biotechnol.* **2015**, *14*, 499–522. [CrossRef]
6. Izadyar, N.; Miller, W. Ventilation Strategies and Design Impacts on Indoor Airborne Transmission: A Review. *Build. Environ.* **2022**, *218*, 109158. [CrossRef]
7. Ye, W.; Zhang, X.; Gao, J.; Cao, G.; Zhou, X.; Su, X. Indoor Air Pollutants, Ventilation Rate Determinants and Potential Control Strategies in Chinese Dwellings: A Literature Review. *Sci. Total Environ.* **2017**, *586*, 696–729. [CrossRef]
8. Chenari, B.; Dias Carrilho, J.; Gameiro Da Silva, M. Towards Sustainable, Energy-Efficient and Healthy Ventilation Strategies in Buildings: A Review. *Renew. Sustain. Energy Rev.* **2016**, *59*, 1426–1447. [CrossRef]
9. Atkinson, J.; Jensen, P. *Natural Ventilation for Infection Control in Health-Care Settings*; World Health Organization: Geneva, Switzerland, 2010; ISBN 9789241547857.
10. Alvarenga, M.O.P.; Dias, J.M.M.; Lima, B.J.L.A.; Gomes, A.S.L.; Monteiro, G.Q.M. The Implementation of Portable Air-Cleaning Technologies in Healthcare Settings—A Scoping Review. *J. Hosp. Infect.* **2023**, *132*, 93–103. [CrossRef]
11. Mata, T.M.; Martins, A.A.; Calheiros, C.S.C.; Villanueva, F.; Alonso-Cuevilla, N.P.; Gabriel, M.F.; Silva, G.V. Indoor Air Quality: A Review of Cleaning Technologies. *Environments* **2022**, *9*, 118. [CrossRef]
12. González-Martín, J.; Kraakman, N.J.R.; Pérez, C.; Lebrero, R.; Muñoz, R. A State–of–the-Art Review on Indoor Air Pollution and Strategies for Indoor Air Pollution Control. *Chemosphere* **2021**, *262*, 128376. [CrossRef]
13. Niu, M.; Shen, F.; Zhou, F.; Zhu, T.; Zheng, Y.; Yang, Y.; Sun, Y.; Li, X.; Wu, Y.; Fu, P.; et al. Indoor Air Filtration Could Lead to Increased Airborne Endotoxin Levels. *Environ. Int.* **2020**, *142*, 105878. [CrossRef]
14. Szabados, M.; Magyar, D.; Tischner, Z.; Szigeti, T. Indoor Air Quality in Hungarian Passive Houses. *Atmos. Environ.* **2023**, *307*, 119857. [CrossRef]
15. De Oliveira, A.E.; Guerra, V.G. Electrostatic Precipitation of Nanoparticles and Submicron Particles: Review of Technological Strategies. *Process Saf. Environ. Prot.* **2021**, *153*, 422–438. [CrossRef]
16. Afshari, A.; Ekberg, L.; Forejt, L.; Mo, J.; Rahimi, S.; Siegel, J.; Chen, W.; Wargocki, P.; Zurami, S.; Zhang, J. Electrostatic Precipitators as an Indoor Air Cleaner—A Literature Review. *Sustainability* **2020**, *12*, 8774. [CrossRef]
17. Parker, K. *Electrical Operation of Electrostatic Precipitators*; The Institution of Electrical Engineers: London, UK, 2007.
18. Vaze, N.; Gold, B.; Lindsey, D.; Moore, M.D.; Koutrakis, P.; Demokritou, P. An Assessment of the Efficacy of Commercial Air Ionizer Systems Against a SARS-CoV-2 Surrogate. *Microorganisms* **2025**, *13*, 593. [CrossRef]
19. Banche, G.; Rita Iannantuoni, M.; Musumeci, A.; Allizond, V.; Maria Cuffini, A. Use of Negative and Positive Ions for Reducing Bacterial Pathogens to Control Infections. *Acta Sci. Microbiol.* **2019**, *2*, 35–38. [CrossRef]
20. Pino, O.; La Ragione, F. There's Something in the Air: Empirical Evidence for the Effects of Negative Air Ions (NAI) on Psychophysiological State and Performance. *Res. Psychol. Behav. Sci.* **2013**, *1*, 48–53. [CrossRef]
21. Terman, M.; Su Terman, J. Article Controlled Trial of Naturalistic Dawn Simulation and Negative Air Ionization for Seasonal Affective Disorder. *Am. J. Psychiatry* **2006**, *163*, 2126–2133. [CrossRef] [PubMed]
22. Iwama, H. Negative Air Ions Created by Water Shearing Improve Erythrocyte Deformability and Aerobic Metabolism. *Indoor Air* **2004**, *14*, 293–297. [CrossRef]
23. Bailey, W.H.; Williams, A.L.; Leonhard, M.J. Exposure of Laboratory Animals to Small Air Ions: A Systematic Review of Biological and Behavioral Studies. *Biomed. Eng. Online* **2018**, *17*, 72. [CrossRef] [PubMed]
24. Wallner, P.; Kundi, M.; Panny, M.; Tappler, P.; Hutter, H.P. Exposure to Air Ions in Indoor Environments: Experimental Study with Healthy Adults. *Int. J. Environ. Res. Public Health* **2015**, *12*, 14301–14311. [CrossRef]
25. Gord, J.; Vigil, C.; Richards, S.; Bertram, T.H. Classroom Scale Measurements of the Efficacy of Ventilation, Filtration, and Electronic Air Cleaners for the Removal of Aerosol Particles. *Build. Environ.* **2023**, *244*, 110758. [CrossRef]
26. Han, T.T.; Mainelis, G. Assessment of Ionization-Type Car Air Purifiers under Actual Driving Conditions. *Aerosol Sci. Technol.* **2025**, *59*, 1289–1301. [CrossRef]
27. Zhang, Q.; Essien, D.; Zhang, K.Y. A Review of Air Ionization with Negative Ions for Aerosol Removal and Inactivation of Airborne Microorganisms in Confined Spaces. *KONA Powder Part. J.* **2026**, *43*, 191–200. [CrossRef]
28. Sobek, E.; Elias, D.A. Bipolar Ionization Rapidly Inactivates Real-World, Airborne Concentrations of Infective Respiratory Viruses. *PLoS ONE* **2023**, *18*, e0293504. [CrossRef] [PubMed]
29. Asada, K.; Yoshimizu, K.; Okano, M. Effects of Position of an Electric Field Shield on the Neutralization Characteristics of a Corona Discharge Air Ionizer. *IEEJ Trans. Electr. Electron. Eng.* **2023**, *18*, 1544–1546. [CrossRef]

30. *ASTM E741-00*; Standard Test Method for Determining Air Change in a Single Zone by Means of a Tracer Gas Dilution. ASTM International: West Conshohocken, PA, USA, 2000.
31. Gilardoni, S.; Massoli, P.; Giulianelli, L.; Rinaldi, M.; Paglione, M.; Pollini, F.; Lanconelli, C.; Poluzzi, V.; Carbone, S.; Hillamo, R.; et al. Fog Scavenging of Organic and Inorganic Aerosol in the Po Valley. *Atmos. Chem. Phys.* **2014**, *14*, 6967–6981. [CrossRef]
32. Ekholm, V.; Caleman, C.; Bjärnhall Prytz, N.; Walz, M.M.; Werner, J.; Öhrwall, G.; Rubensson, J.E.; Björneholm, O. Strong Enrichment of Atmospherically Relevant Organic Ions at the Aqueous Interface: The Role of Ion Pairing and Cooperative Effects. *Phys. Chem. Chem. Phys.* **2018**, *20*, 27185–27191. [CrossRef]
33. Psomas, T.; Teli, D.; Langer, S.; Wahlgren, P.; Wargocki, P. Indoor Humidity of Dwellings and Association with Building Characteristics, Behaviors and Health in a Northern Climate. *Build. Environ.* **2021**, *198*, 107885. [CrossRef]
34. Grinshpun, S.A.; Mainelis, G.; Trunov, M.; Adhikari, A.; Reponen, T.; Willeke, K. Evaluation of Ionic Air Purifiers for Reducing Aerosol Exposure in Confined Indoor Spaces. *Indoor Air* **2005**, *15*, 235–245. [CrossRef] [PubMed]
35. Voccio, J.; Zenouzi, M.; Seredinski, A.; Khabari, A.; Young, S.; Reddick, T.; Lanzrath, A.; Weekes-Tulloch, A.; Almonte, M.; Ruci, J.; et al. Experimental Study of Aerosol Behavior in Ambient Electric and Magnetic Fields at Low Indoor Relative Humidity. *J. Electrost.* **2024**, *130*, 103937. [CrossRef]
36. Romay, F.J.; Ou, Q.; Pui, D.Y.H. Effect of Ionizers on Indoor Air Quality and Performance of Air Cleaning Systems. *Aerosol Air Qual. Res.* **2024**, *24*, 230240. [CrossRef]
37. Nunayon, S.S.; Zhang, H.H.; Jin, X.; Lai, A.C. Experimental Evaluation of Positive and Negative Air Ions Disinfection Efficacy under Different Ventilation Duct Conditions. *Build. Environ.* **2019**, *158*, 295–301. [CrossRef]
38. Ling, X.; Jayaratne, R.; Morawska, L. Air Ion Concentrations in Various Urban Outdoor Environments. *Atmos. Environ.* **2010**, *44*, 2186–2193. [CrossRef]
39. Li, X.; Gupta, D.; Eom, H.J.; Kim, H.K.; Ro, C.U. Deliquescence and Efflorescence Behavior of Individual NaCl and KCl Mixture Aerosol Particles. *Atmos. Environ.* **2014**, *82*, 36–43. [CrossRef]
40. Chuang, H.C.; Jones, T.; Chen, Y.; Bell, J.; Wenger, J.; Bérubé, K. Characterisation of Airborne Particles and Associated Organic Components Produced from Incense Burning. *Anal. Bioanal. Chem.* **2011**, *401*, 3095–3102. [CrossRef]
41. Vu, T.V.; Ondracek, J.; Zdímal, V.; Schwarz, J.; Delgado-Saborit, J.M.; Harrison, R.M. Physical Properties and Lung Deposition of Particles Emitted from Five Major Indoor Sources. *Air Qual. Atmos. Health* **2017**, *10*, 1–14. [CrossRef]
42. Pushpawela, B.; Jayaratne, R.; Nguy, A.; Morawska, L. Efficiency of Ionizers in Removing Airborne Particles in Indoor Environments. *J. Electrost.* **2017**, *90*, 79–84. [CrossRef]
43. Kwok, P.C.L.; Chan, H.K. Effect of Relative Humidity on the Electrostatic Charge Properties of Dry Powder Inhaler Aerosols. *Pharm. Res.* **2008**, *25*, 277–288. [CrossRef] [PubMed]
44. Kolarž, P.; Ilić, A.; Janković, M.; Janićijević, A.; Trbovich, A.M. Estimating Aerosol Particle Removal in Indoor Air by Ion-Enhanced Deposition. *J. Aerosol Sci.* **2023**, *173*, 106199. [CrossRef]
45. Zeng, Y.; Manwatkar, P.; Laguerre, A.; Beke, M.; Kang, I.; Ali, A.S.; Farmer, D.K.; Gall, E.T.; Heidarinejad, M.; Stephens, B. Evaluating a Commercially Available In-Duct Bipolar Ionization Device for Pollutant Removal and Potential Byproduct Formation. *Build. Environ.* **2021**, *195*, 107750. [CrossRef]
46. Zeng, Y.; Heidarinejad, M.; Stephens, B. Evaluation of an In-Duct Bipolar Ionization Device on Particulate Matter and Gas-Phase Constituents in a Large Test Chamber. *Build. Environ.* **2022**, *213*, 108858. [CrossRef]
47. Ohsawa, A.; Nomura, N. Continuously Balanced Pulse-DC Ioniser to Minimise the Offset Voltage. *J. Electrost.* **2016**, *79*, 16–19. [CrossRef]
48. Ohsawa, A. Charge Neutralisation: A Review—How Can Corona Ionisers Achieve Zero Coulomb and Zero Volt Charge Neutralisation? *J. Electrost.* **2025**, *137*, 104096. [CrossRef]
49. Shi, B.; Ekberg, L. Ionizer Assisted Air Filtration for Collection of Submicron and Ultrafine Particles-Evaluation of Long-Term Performance and Influencing Factors. *Environ. Sci. Technol.* **2015**, *49*, 6891–6898. [CrossRef] [PubMed]
50. Nazaroff, W.W. Residential Air-Change Rates: A Critical Review. *Indoor Air* **2021**, *31*, 282–313. [CrossRef]
51. Božič, A. Relationship between Indoor and Outdoor Temperature and Humidity in a Residential Building in Central Europe. *Discov. Environ.* **2024**, *2*, 63. [CrossRef]
52. Fletcher, L.A.; Noakes, C.J.; Sleigh, P.A.; Beggs, C.B.; Shepherd, S.J. Air Ion Behavior in Ventilated Rooms. *Indoor Built Environ.* **2008**, *17*, 173–182. [CrossRef]
53. Farahi, F. Soft Ionization: Improving Indoor Air Quality. *IEEE Trans. Ind. Appl.* **2023**, *59*, 5580–5586. [CrossRef]
54. Černecký, J.; Valentová, K.; Pivarčiová, E.; Božek, P. Ionization Impact on the Air Cleaning Efficiency in the Interior. *Meas. Sci. Rev.* **2015**, *15*, 156–166. [CrossRef]